Orientum-Occidentum
© Bejoy Narayan Mahavidyalaya
url: https://bnmv.ac.in/college_journal.php

Vol. 1 No. 1, 33-40 (2022)

DEFECT-DYNAMICS AND NON-CONVENTIONAL FERROMAGNETISM IN NONMAGNETIC K-SUBSTITUTED ZnO NANOWIRES

Shyamsundar Ghosh

Department of Physics, Bejoy Narayan Mahavidyalaya, Itachuna, Hooghly 712 147, India

Email: sghoshphysics@gmail.com

Abstract

Nanowires of Zn1-xKxO have been fabricated by an easy wet chemical template assisted route by using nanoporous anodic aluminium oxide as template. Cation vacancy-induced d0 ferromagnetism is observed in all undoped and K-doped ZnO nanowires. Ferromagnetic signature was found to increase with increasing K-concentration having a maximum moment of ~ 2.1 emu/cm3 for x = 0.04 and then decreased on further K-doping. Presence of large amount of zinc vacancies were observed from photoluminescence spectral analysis. The substitution of K at Zn site might have favoured to stabilize Zn vacancies and the magnetic moment of Zn vacancy defects are mediated by holes due to K-substitution at Zn site and thus stabilize ferromagnetic interaction. This study demonstrates that the ferromagnetism in ZnO nanowires can be tuned by controlling cation vacancies using proper dopant.

1. Introduction

Defect-induced FM in wide-band oxides has recently drawn immense attention as a new class of dilute magnetic semiconductors (DMS's) for spintronic application [1]. After the theoretical prediction by T. Deitl et al. [2], different controversial results were reported regarding the presence or absence of intrinsic ferromagnetism (FM) in conventional transition metal (TM) or rare earth element (RE) doped oxide semiconductors [3-4]. However, the observation of room-temperature

FM in pure HfO2 thin films by Venkatesan et al. [5] has opened up a new phenomenon, so-called d0 FM. The ab-initio calculations performed by Pemmaraju et al. [6] for HfO2 that cationic vacancies can induce an almost localized magnetic moment on the oxygen atoms neighboring the vacancy. In contrast, in case of oxygen vacancy (anion vacancy) leads to the absence of magnetic moment. The name "d0 FM" suggests that magnetism is not originating from unpaired d-orbital but from p-orbital's of neighboring anions adjacent to cation vacancy.

In 2006, Hong et al. [7] suggested that structural defects might induce d0 FM in insulating TiO2, In2O3 and HfO2 thin films where the magnetization depends on the thickness of films. Recently, first-principles density functional theory (DFT) based calculation has shown that Zn vacancy (VZn) has almost localized magnetic moment of ~ 1.33 μB [8]and doping of proper elements in ZnO thin films can stabilize VZn and introduces holes at the same time, which generate ferromagnetic ordering in the material. Extensive theoretical calculations by Wang et al. [9] showed that the magnetism in ZnO thin films and NWs are due to VZn instead of oxygen vacancy (VO) and they also suggested that VZn generally prefers to reside at surface. In our earlier studies, we have invested d0 FM originated from oxygen vacancy [10, 11] in oxide thin-films but stabilization of cation vacancy-induced FM in oxide nanostructures with proper control can have much impact in the field of spintronic devices. Therefore, here, we have fabricated pure ZnO nanowires (NWs) by an easy wet chemical template assisted route using nanoporous anodic aluminium oxide (AAO) as template. As-prepared undoped ZnO NWs exhibit room-temperature FM. This ferromagnetism is controlled by doping with potassium (K) and it is found that up-to a certain K concentration the FM signature increases and decreases after that. The origin of the enhanced magnetization in K-doped ZnO NWs has been investigated by correlating the photoluminescence (PL) results with magnetic measurements. The studies indicate that doing with K plays a crucial role to stabilize VZn related defects and to induce FM in K-doped ZnO NWs. Hence, the possibility of tailoring the magnetic properties in K-doped ZnO NWs by controlling the cation vacancies with proper doping can open new horizon in spintronics.

2. Experimental details

Pristine and K-doped ZnO NWs were fabricated within the pores of the AAO by employing a simple wet chemical method. The arrays of ZnO NWs were grown by dipping the template into a saturated 0.1 M solution of Zn(CH3COOH)2•2H2O prepared in ethanol followed by drying and annealing of the template. In order to fabricate 2, 4 and 8 at. % K-doped ZnO NWs selective amount of potassium acetate was added in the zinc acetate solution in appropriate ratios. After the formation of NWs, AAO template was partially dissolved in 2 M NaOH solution to release the NWs to study the morphology of the NWs by field emission scanning electron microscope (FESEM). The chemical composition of the NWs was determined by energy dispersive x-ray (EDAX)analysis. X-ray diffraction (XRD) was used to obtain the crystallographic information of the template embedded un-doped and K-doped ZnO NWs. Room temperature Photoluminescence (PL) measurements of the template embedded NWs were conducted by using a spectrofluorometer (Horiba Jobin Yvon, Fluorolog-3) having Xe lamp source with an excitation wavelength of 330 nm. Magnetic measurements of the aligned arrays of template embedded un-doped and K-doped

ZnO NWs were carried out by using a vibrating sample magnetometer (VSM, Lakeshore, model 7144) in the temperature range of 80 to 550 K.

3. Results and discussions

3.1 Structural analysis

Figure 1(a) shows the representative FESEM image of the AAO template within which un-doped and K-doped ZnO NWs were grown. It shows that template has average pore diameters of ~ 40-45 nm. The low magnification FESEM image of 4% K doped ZnO NWs is shown in figure 1(b) and figure 1(c) shows high magnification FESEM images of the discrete NWs. The diameter of K doped ZnO NWs is about 40 nm, which is found to be very close to the diameter of the pores of the AAO. The corresponding on-spot EDAX spectra of the same NWs are shown in figure 1 (d) which shows the elemental compositions.

XRD patterns of un-doped and K-doped ZnO NWs are shown in Fig. 1(e), which indicates hexagonal wurztite crystal structure of NWs which are polycrystalline in nature. The lattice parameters of the hexagonal unit cell for all K-doped ZnO NWs are estimated using Bragg's diffraction law. The variation of lattice parameters (a and c-parameters) are plotted in inset of Fig. 1(e). Both the lattice parameters a and c are found to increase almost linearly with K concentration, which ascertains the substitution of K ions replacing Zn ions. However, a close inspection shows that the change in c-parameter is more rapid than a-parameter. The result indicates that the majority of K ions are substituted along c-axis of the unit cell resulting significant elongation of the c-parameter. The expansion of lattice parameters is due to the substitution of large K1+ ions (151 pm) replacing the smaller Zn2+ ions (74 pm). The strong diffraction peaks at 2θ values of 38.48 and 44.84 appear from the electropolished Al substrate underneath AAO.

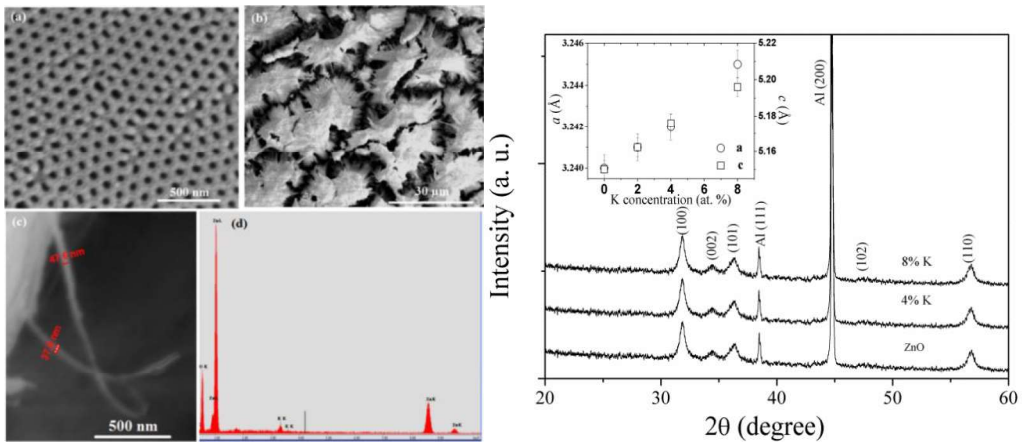

Figure 1. (a) FESEM images of blank AAO template. (b) low and (c) high magnification FESEM images of 4% K-doped ZnO NWs partially released from AAO. (d) Corresponding on-spot EDAX spectra (e) XRD patterns of un-doped, 4% and 8% K-doped ZnO NWs. Inset: Lattice parameters (a and c) of K-doped ZnO NWs as a function of K-concentration.

3.2 Green emission in photoluminescence spectra

Room temperature PL spectra of the as prepared pure and K-doped ZnO NW subtracting AAO template contribution are shown in Fig. 3. Both the un-doped and K-doped ZnO NWs provide a UV emission near 385 nm, which is attributed to the near band edge (NBE) electronic transition and/or the free exciton recombination through an exciton–exciton collision process [12]. It is evident that K-doping increases the sharpness of the NBE UV emission. The other prominent emission peaks are observed for K-doped ZnO NWs in blue (450 and 468 nm), blue-green (481 nm), green (510 nm) and yellow-orange (615 nm) zones. The blue emission can be attributed due to K impurity related defects such as K- interstitial (Ki) and K-substitutional (KZn) [13] while the blue-green (~2.53 eV) and yellow-orange (~ 2.02 eV) can be attributed to O vacancies and O interstitial [14]. The origin of the green emission (2.44 eV) of K-doped ZnO NWs is mainly related to the VZn [14-16]. It is interesting to notice that in our case, the intensity of the green luminescence peak (IG) of the pure ZnO NWs is significantly low. On the other hand, the green emission peak becomes sharper in case of the K-doped ZnO NWs and its intensity increases with the increase of the K concentration up to 4 % K-doping and then decreases. It is reported that the VZn have low formation energy under n-type conditions [15], which indicates that the annealing in O-rich atmosphere promotes the formation of VZn. Therefore, in our case, formation of VZn in un-doped ZnO NWs is quiet expected. Recently, Yi et al [8] demonstrated that the formation energy of the VZn decreases because of Li doping in ZnO matrix and hence the VZn are stabilized [15]. Similarly, K-doping in ZnO NWs might promote the formation of more VZn and hence exhibit strong green luminescence. The 4% K-doped ZnO NWs exhibit strongest green luminescence characteristic which indicates the presence largest amount of VZn among the all K-doped ZnO NWs samples.

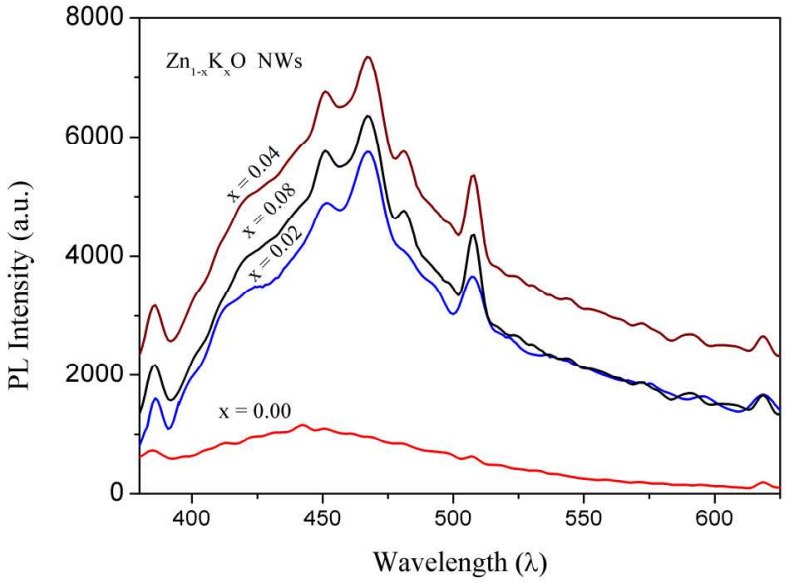

Figure 2. Room-temperature photoluminescence spectra for pristine and K-doped ZnO NWs.

3.3 Non-conventional ferromagnetism

The magnetic hysteresis (M-H) loops of the un-doped and 4% K-doped ZnO NWs are shown in Fig. 4 (a) and (b) for 300 and 80 K, respectively. It is evident that the un-doped ZnO NWs exhibit FM both at room and low temperature. Interestingly, ferromagnetic response is found to enhance after K-doping in ZnO NWs. The saturation magnetization (Ms) increases initially with the increase of K concentration upto 4 % K-doping and then decreases with further doping (Fig. 4 (c)). The maximum saturation magnetization (Ms) of 2.1 and 4.5 emu cm-3 has been obtained for 4 % K-doped ZnO NWs at T = 300 and 80 K, respectively. Figure 4(d) shows the temperature dependence of magnetization of the un-doped and 4% K-doped ZnO NWs. The Curie temperature (Tc) of un-doped and 4% K-doped ZnO NWs is 386 and 516 K, respectively. The variation of Tc with K concentration is shown in the inset of figure 4(e). It is found that the Tc of the K-doped ZnO NWs also increases with the increase of K concentration in ZnO NWs up to 4% K-doping and then decreases with further doping, which follows the similar trend of the saturation magnetization. Therefore, an optimum K-concentration of 4% can be defined, where ferromagnetic response of K-doped ZnO NWs became strongest.

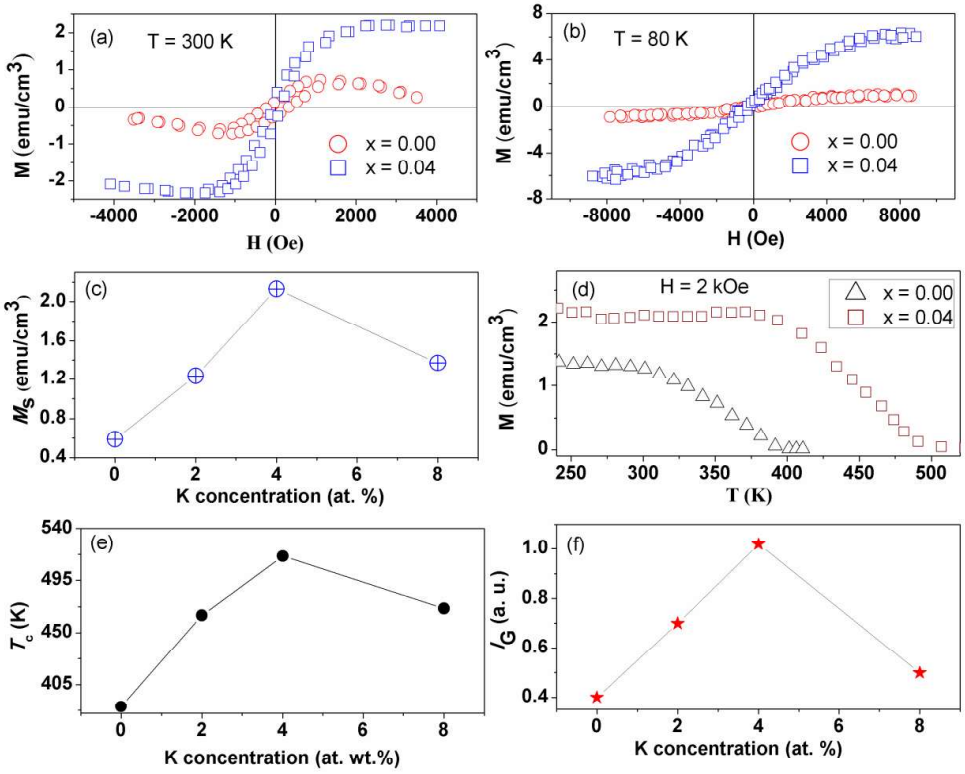

Figure 3. M-H loops of Zn1-xKxO NWs at (a) 300 K and (b) 80 K. (c) Saturation magnetization as a function of K-concentration (at.%). (d) M (T) curve for K-doped ZnO NWs. (e) Estimated Curie temperature and (f) Relative Green luminescence intensity (IG) obtained from PL spectra of K-doped NWs as function of K-concentration (at.%).

3.4 Origin of Non-conventional ferromagnetism

As far as the origin of ferromagnetism in the pristine and K-doped ZnO NWs is concern, VZn defects might be favourable cause. This kind of cation vacancy defects can grow in the ZnO NWs during its fabrication through annealing at high temperature under oxygen rich condition and their signature is also confirmed from the PL measurements. However, in ZnO, VO is also a common defect and the VO clusters can also introduce moments in the system [17-18]. Therefore, the influence of VO clusters in the FM of ZnO NWs is also considerable. Although in our experiment the major contribution to the ferromagnetic response of the ZnO NWs is believed to be due to the presence of cation vacancies (VZn). However, an interesting correlation between the nature of Ms and the green emission intensity (IG) should be noticed for the K-doped ZnO NWs, where both of them increases with the increase of K-concentration in ZnO up to 4% K-doping (see Fig. 4 (c) and (f)). This correlation fairly suggests that the observed FM is related to the VZn concentration. Additionally, earlier PL measurements of K-doped ZnO NWs (see Fig. 3) indicate that significant amount of KZn and/or Ki defects are present in the NWs. Therefore, formation of defect combination like KZn and/or Ki lowers the formation energy of each Zn vacancy and hence stabilizes VZn, similar to the case of Li-doped ZnO thin films [8]. With the increase of K-doping in ZnO NWs more KZn and/or Ki defects are likely to form and hence more VZn are grown (evident from PL spectra), which results into enhancement in the magnetization. The 4% K-doped ZnO NWs have largest amount of K related defects as well as VZn defects. Therefore, the 4% K-doped ZnO NWs exhibit the strongest FM signature because of presence of large concentration of VZn.

It has been reported that the magnetic moment in the ZnO NWs is not originated from Zn 3d-orbital but from unpaired 2p electrons of O atom in the immediate vicinity of VZn [9]. The substitutional defects (like KZn) originated due to the doping of group-I elements as well as the VZn introduce holes in the system and ferromagnetic interaction can be mediated by these holes between the magnetic moments of VZn [8] to have a long range interaction. The model proposed by Bouzerer and Ziman [19] have shown the dependency of vacancy-induced local magnetic moment and magnetic coupling required by long–range ordering described via a single correlated band of oxygen orbitals with additional random potentials. This type of potential arises due to the substitutional defects and density of vacancies present in the matrix. They predicted that a well-defined region of potential, defect concentration, as well as carrier density exists where the FM with high temperature is possible with few percentages of vacancies or substitutional defects like Li, Na, K etc. Beyond the optimum window of defect concentration, magnetic moment as well as Tc vanishes as the magnetic couplings are destroyed by Rudermann-Kittel-Kaysa-Yashida type oscillations or antiferromagnetic superexchange. Here in our case we have also observed that up to 4% K-doping Tc increases and then decreases on further K-doping. With the increase of K-doping in ZnO the hole concentration should increase in the matrix and after an optimum hole concentration the ferromagnetic ordering is destroyed gradually resulting in decrease of magnetic moment as well as Tc beyond 4%-K doped ZnO NWs.

Conclusion

Zn1-xKxO NWs have been successfully fabricated within the pores of the AAO template by employing a simple wet chemical route. K-doped ZnO NWs exhibit enhanced RT luminescence in the green and blue-green regions, which are ascribed to the VZn and K-related defects, respectively. The expansion of lattice volume with K-doping in ZnO NWs supports the substitution of K ions replacing the Zn ions of the host. Both the un-doped and K-doped ZnO NWs exhibit d0 RTFM. The ferromagnetic response of the ZnO NWs is found to enhance on K-doping. Magnetization increases proportionally with K-doping up to a certain K concentration (4%) and decreases on further K-doping. The observed correlation between the green emission peak intensity (IG) and saturation magnetization (Ms) suggests that Zn vacancy-induced d0 FM in ZnO NWs can be stabilized by K-doping. The study indicates the possibility of tailoring the magnetic properties of ZnO nanostructures by controlling the cation vacancies using suitable dopant and can found to be very promising to fabricate ZnO based defect-engineered DMS devices.

Acknowledgements

The author is thankful to Prof. Kalyan Mandal, S. N. Bose National Centre for Basic Sciences, Kolkata for providing laboratory facilities during the course of this work.

References

[1] H. Ohno, “Making nonmagnetic semiconductors ferromagnetic,” *Science* 281 951 **(1998)**

[2] T. Dietl, H. Ohno, F. Matsukura, J. Cibert and D. Ferrand, “Zener model description of ferromagnetism in zinc-blende magnetic semiconductors,” *Science* 287, 1019 **(2000).**

[3] A. Zunger, S. Lany and H. Raebiger, “The quest for dilute ferromagnetism in semiconductors: guides and misguides by theory”, *Physics*, 3, 53 **(2010).**

[4] S. Ghosh, D. De Munshi and K. Mandal, “Paramagnetism in single-phase Sn1−xCoxO2 dilute magnetic semiconductors,” *J. Appl. Phys*., 107, 123919 **(2010).**

[5] M.Venkatesan, C. B. Fitzgerald and J. M. D. Coey, “Unexpected magnetism in a dielectric oxides” *Nature*, 430, 630 **(2004).**

[6] C. D. Pemmaraju and S. Sanvito, “FM driven by intrinsic point defects in HfO2” *Phys. Rev. Lett*.94, 217205 **(2005)**.

[7] N. H. Hong, J. Sakai, N. Poirot and V. Brizé, "Room-temperature ferromagnetism observed in undoped semiconducting and insulating oxide thin films," *Phys. Rev. B* , 73, 132404 **(2006).**

[8] J. B. Yi, C. C. Lim, G.Z. Xing, H. M. Fan, L.H. Van, S. L. Huang, K.S. Yang, X. L. Huang, X. B. Qin, B.Y.Wang, T. Wu, L. Wang, H. T. Zhang, X. Y. Gao, T. Liu, A. T. S. Wee, Y .P. Feng and J. Ding, "Ferromagnetism in dilute magnetic semiconductors through defect engineering: Li-doped ZnO," *Phys. Rev. Lett*., 104, 137201 **(2010)**.

[9] Q. Wang, Q. Sun, G. Chen, Y. Kawazoe and P. Jena, "Vacancy-induced magnetism in ZnO thin films and nanowires" *Phys Rev. B*,77, 205411 **(2008)**.

[10] G. G. Khan, S. Ghosh, A. Sarkar, G. Mandal, G. D. Mukherjee, U. Manju, N. Banu, and B. N. Dev, "Defect-engineered d0 ferromagnetism in tin-doped indium oxide nanostructures and nanocrystalline thin-films" *Journal of Applied Physics* 118, 074303 **(2015)**.

[11] S. Ghosh and B. N. Dev, "Probing of O2 vacancy defects and correlated magnetic, electrical and photoresponse properties in indium-tin oxide nanostructures by spectroscopic techniques" *Applied Surface Science*, 439, 891–899 **(2018)**

[12] Y. C. Kong, D. P. Yu, B. Zhang, W. Fang and S. Q. Feng, "Ultraviolet-emitting ZnO nanowires synthesized by a physical vapor deposition approach," *Appl. Phys. Lett*., 78, 407 **(2001).**

[13] L. Xu, X. Li and J. Yuan, "Effect of K-doping on structural and optical properties of ZnO thin films," *Superlattices and Microstructures*, 44, 276–281 **(2008)**.

[14] T. Moe Børseth, B. G. Svensson and A. Yu. Kuznetsov, "Identification of oxygen and zinc vacancy optical signals in ZnO," *Appl. Phys. Lett*.89, 262112 **(2006).**

[15] A. Janotti and C. G. Van de Walle, "Fundamentals of zinc oxide as a semiconductor," *Rep. Prog. Phys*., 72, 126501 **(2009)**.

[16] A. F. Kohan, G. Ceder, D. Morgan and C. G. Van de Walle, "First-principles study of native point defects in ZnO," *Phys. Rev. B*, 61, 15019 **(2000).**

[17] S. Ghosh and P.M.G. Nambissan, "Evidence of oxygen and Ti vacancy induced ferromagnetism in post-annealed undoped anatase TiO2 nanocrystals: A spectroscopic analysis" *Journal of Solid State Chem*. 275, 174–180 **(2019).**

[18] R. Podila, W. Queen, A. Nath, J. T. Arantes, A. L. Schoenhalz, A. Fazzio, G. M. Dalpian, J. He, S. J . Hwu, M. J. Skove and A. M. Rao, Origin of FM ordering in pristine micro- and nanostructured ZnO," *Nano Lett*., 10, 1383 **(2010).**

[19] G. Bouzerar and T. Ziman, "Model for vacancy-induced d0 ferromagnetism in oxide compounds," *Phys. Rev. Lett*. 96, 207602 **(2006).**